European Journal of Pharmaceutics and Biopharmaceutics 137 (2019) 196–208

Contents lists available at ScienceDirect

European Journal of Pharmaceutics and Biopharmaceutics

journal homepage: www.elsevier.com/locate/ejpb

Research paper

Modeling, design and manufacture of innovative floating gastroretentive drug delivery systems based on hot-melt extruded tubes

Fabian J. Simons, Karl G. Wagner*

Department of Pharmaceutical Technology and Biopharmaceutics, University of Bonn, Bonn, Germany

ARTICLE INFO

Keywords:
Gastroretentive
Floating
Hot-melt extrusion
Tube extrusion
Drug delivery
Controlled release
Metformin

Chemical compounds studied in this article:
Metformin hydrochloride (PubChem CID: 14219)

ABSTRACT

The problem of many gastroretentive systems is the mechanistic connection of drug release and gastric retention control. This connection could be successfully separated by formulating hollow tubes via hot-melt extrusion and sealing both tube ends, which led to immediately floating devices. The tube wall consisted of metformin crystals embedded in an inert polymer matrix of Eudragit® RS PO and E PO. Very high drug loadings of up to 80% (w/w) were used without generating a 'burst release'. Sustained release profiles from four to more than twelve hours were achieved by varying the polymer proportions without affecting the floatability. Buoyancy was found to mainly depend on the cylinder design, i.e. the outer to inner diameter ratio. This allowed the polymer/metformin composition to be changed without affecting buoyancy, i.e. a separation of floatability and release control was achieved. A prediction model was implemented that allowed for the buoyancy force to be determined with high accuracy by selecting a suitable ratio of outer to inner diameter of the modular tube die. Wall thickness and mass normalized surface area were identified as geometric parameters that mainly influenced the release properties. Conclusively, this study offers a highly flexible and rational manufacturing approach for the development of gastroretentive floating drug delivery systems.

1. Introduction

The development of gastroretentive drug delivery systems (GRDDS) is complex, since a prolonged gastric residence time over the entire release period in combination with a sustained release profile must be ensured. Small liquid amounts and housekeeper waves (propulsive contractions) in the fasted state represent the main challenge for remaining a GRDDS in the stomach [1–3]. In addition, the properties of the gastric fluid vary widely in terms of pH, viscosity and enzyme levels depending on fasted or fed state [4–6]. Ensuring a robust release in a highly fluctuating environment is the other major obstacle [7]. The reasons to start a rather challenging development of a GRDDS are mainly: A narrow absorption window in the upper gastrointestinal tract as described e.g. for Levodopa [8,9], Gabapentin [10,11] and Furosemide [12,13]. The demand for a local therapy in the stomach e.g. during a *Helicobacter pylori* infection [14,15]. Or an increased therapeutic efficiency overcoming low bioavailability and high absorption variability caused by fast gastric transit time [16–19]. Gastroretentive functionality has been established using various approaches. Mainly swelling/size enlargement [8,20], bioadhesion [21,22] and floating principles as well as combinations thereof [23,24] are applied. In order to reduce complexity during GRDDS development, our aim was to separate gastroretentive properties from extended release control. An inert matrix system, in combination with the floating approach seemed to offer more development opportunities, compared to swelling matrix (usually hydrophilic matrices) or bio-adhesive approaches. Hence, the focus of our work was on floating devices, only.

Sodium bicarbonate has been used in various formulations in order to generate carbon dioxide *in situ*, which is subsequently trapped by an impermeable polymer layer, thereby generating the required buoyancy [15,25–27]. However, studies focused on the effect of sodium bicarbonate on the API dissolution behavior showed that the amount of

Abbreviations: API, active pharmaceutical ingredient; CO_2, carbon dioxide; dl, drug load; ds, dose strength; EPO, Eudragit® E PO; EuRS, Eudragit® RS PO; f_1, difference factor; f_2, similarity factor; F_{buoy}, buoyancy force; f_{cor}, correction factor; FDDS, floating drug delivery system; F_{grav}, gravity force; F_{res}, resultant force; GRDDS, gastroretentive drug delivery system; HCL, hydrochloric acid; m_{FDDS}, mass of dosage form; HME, hot-melt extrusion; ID, inner diameter; Met, metformin hydrochloride; OD, outer diameter; ρ_a, apparent density; ρ_d, desired density of sealed extrudates; ρ_{FDDS}, apparent density of dosage form; ρ_p, final blend true density; ρ_s, solvent density; ρ_t, true density; rpm, revolutions per minute; Sa, stearyl alcohol; SEM, scanning electron microscopy; SD, standard deviation; V_{in}, cavity volume; V_{out}, cylinder wall volume; V_{tot}, total volume; XRPD, X-ray powder diffraction

* Corresponding author.
E-mail address: karl.wagner@uni-bonn.de (K.G. Wagner).

https://doi.org/10.1016/j.ejpb.2019.02.022
Received 29 November 2018; Received in revised form 23 February 2019; Accepted 26 February 2019
Available online 28 February 2019
0939-6411/

generated carbon dioxide considerably influences the release rate [15,25,28,29]. Porous tablets were manufactured by incorporation of excipients which could undergo sublimation e.g. menthol, which was removed after tableting under vacuum [30,31]. Hydrodynamically balanced systems as a sub-type of non-effervescent systems have been studied by Enri et al. and Ali et al. [32,33]. The approaches described above, require the polymer to control the release rate and guarantee the floatability. Consequently, varying the sustained release polymer quantity can result in an increased floating lag time or an insufficient floating duration [28,34,35]. In another approach 3D-printing was used to print low density lattice internal structure tablets of dipyridamole, which stayed buoyant for more than 8 h [36]. Floating microspheres manufactured via solvent evaporation were investigated by Kumaraswamy et al. [37]. However, drug loadings of less than 20% were achieved with those two methods. Tablet modules consisting of hydrophilic polymers have been developed, which can be stacked together similar to LEGO bricks creating a cavity between both parts (Dome Matrix®), thus allowing the assembled tablet to float [38]. However, compression of those specially shaped tablet parts and assembling thereof, is very demanding and difficult to automate. As inert matrix tablets exhibit remaining porosity, drug release rates will be faster compared to hot-melt extruded matrices of almost zero porosity [39]. Thus, higher drug loads are likely to be achieved by extrusion compared to compressed inert matrix tablets due to a higher extended release capacity. However, hot-melt extrusion (HME), as a versatile alternative to conventional production methods, has been barely investigated for the manufacture of floating drug delivery systems (FDDS) [40,41]. Porous extrudates have been manufactured using the thermal decomposition of sodium bicarbonate to generate CO_2 during extrusion in order to obtain a sponge-like structure [42]. Vo et al. evaluated foamed-structure pellets by liquid injection of ethanol during extrusion and subsequent liquid-vapor phase transition [43]. Nakamichi et al. prepared puffed extrudates by implementing high pressure screw elements close to the die to provoke extensive die swelling [44]. Vo et al. combined the thermal decomposition of sodium bicarbonate to form a porous structure with the bio-adhesive properties of hydroxypropyl cellulose to obtain a dual-mechanism gastroretentive system [45]. Ensuring a specific pore size distribution in porous floating systems produced via HME is very challenging particularly because the pore size depends on a variety of factors, e.g. temperature, pressure and sodium bicarbonate particle size [30]. Consequently, the development of porous or gas-generating floating systems is always a compromise between floating ability and sustained release properties.

The aim of the present work was to establish a floating device where release control is provided by an inert matrix at almost zero porosity, i.e. a high extended release capacity. We selected the tube extrusion approach as a highly advantageous direct shaping technique to produce hollow, floating gastroretentive drug delivery systems. The cylinder wall acted as the inert matrix system built by dispersed metformin crystals in an inert polymer. The cylindrical geometry of these hollow systems enabled a separation of floating ability and release properties. The buoyancy depended mainly on the volume ratio between cylinder wall and hollow cavity. Therefore, the cylinder wall composition can be varied while the floating behavior should be only slightly affected. Metformin hydrochloride (Met) was used as a model drug. Met is a well-known API for first-line treatment of type II diabetes. Met is highly water soluble, but exhibits a narrow absorption window in the upper gastrointestinal tract with saturable and dose-dependent uptake [46–48]. Therefore, Met would highly benefit from a sustained release system, which due to its narrow absorption window should incorporate a gastroretentive mechanism [49]. To date, only one gastroretentive system is commercially available for Metformin (Glumetza®), which is based on a swelling and size enlargement principle [50,51].

2. Material and methods

2.1. Material

Metformin hydrochloride (Met) with a d_{50} of 55 µm and a d_{90} of 127 µm was obtained from Wanbury Limited (Mumbai, India) [52]. Ammonio Methacrylate Copolymer, Type B (Eudragit® RS PO, EuRS), Basic Butylated Methacrylate Copolymer (Eudragit® E PO, EPO) and Aerosil® 200 Pharma were kindly provided by Evonik Industries AG (Darmstadt, Germany). Stearyl alcohol (Sa) was purchased from Carl Roth GmbH + Co. KG (Karlsruhe, Germany). Polyvinylacetate (Vinnapas® B17 spezial) was obtained from Wacker Chemie AG (Munich, Germany).

2.2. Preparation of physical mixtures

Prior to the manufacturing process, stearyl alcohol flakes were cryo-milled 3 × 30 s at 30 Hz using a MM 400 ball mill (Retsch GmbH, Haan, Germany). Subsequently, Eudragit RS, Eudragit E and milled stearyl alcohol were blended in a Turbula blender (Willy A. Bachofen AG Maschinenfabrik, Germany) for 5 min at 50 rpm to form the *pre-blend*. Metformin and Aerosil were passed through a 500 µm and 250 µm sieve respectively in order to break down agglomerates and ensure a homogenous particle size distribution. In a final step, both ingredients were added to the *pre-blend* and mixed in the Turbula blender for additional 10 min at 50 rpm to obtain the *final blends* (Table 1, Met 1–10). The batch size was 80 – 100g.

2.3. Manufacturing of hollow extrudates

Fig. 1 shows schematically the manufacturing process of hollow floating delivery systems using hot-melt tube extrusion. The process was performed with a co-rotating 12 mm twin-screw extruder ZE 12 (Three-Tec GmbH, Seen, Switzerland) with a functional length of 25:1 L/D. Two kneading areas (30°+ 60° and 60°+ 90°) were mounted to ensure a homogenous API distribution within the polymer matrix. The extruder was equipped with a modular design tube die to obtain different outer (OD) to inner (ID) diameter ratios. The die outlet was aligned vertically to avoid collapse of the tube by gravitation. The die tip and die plate could be varied in 1 mm steps respectively (ID: 3, 4, 5, 6 mm; OD: 6, 7, 8, 9 mm). The used die combination of each respective batch is given in brackets (OD/ID). Throughput was kept constant at 120 g/h and screw speed was set to 100 rpm for all trials. Stearyl alcohol was added as a plasticizer to mixtures with high drug load (≥ 70%) in order to reduce torque during manufacture and ensure processability. The temperature profile for extrusion was adjusted within the range of 120–140 °C defined by the extrudate properties (to avoid tube collapse) and extruder torque. The applied extrusion temperatures are listed in the supplementary data (Table A.2). Obtained extrudate tubes were cooled to room temperature and cut into small cylinders. The length varied in the range of 13 – 20 mm depending on the

Table 1
Composition of extrudate formulations evaluated in the present study (w/w %).

Sample	Metformin [%]	EuRS [%]	EPO [%]	Sa [%]	Aerosil [%]
Met 1	69.5	27	0	3	0.5
Met 2	69.5	27	0	3	0.5
Met 3	69.5	20.2	6.8	3	0.5
Met 4	69.5	13.5	13.5	3	0.5
Met 5	69.5	10.8	16.2	3	0.5
Met 6	69.5	6.8	20.2	3	0.5
Met 7	50	37.5	12.5	0	0
Met 8	50	25	25	0	0
Met 9	50	35	15	0	0
Met 10	79.5	18	0	2	0.5

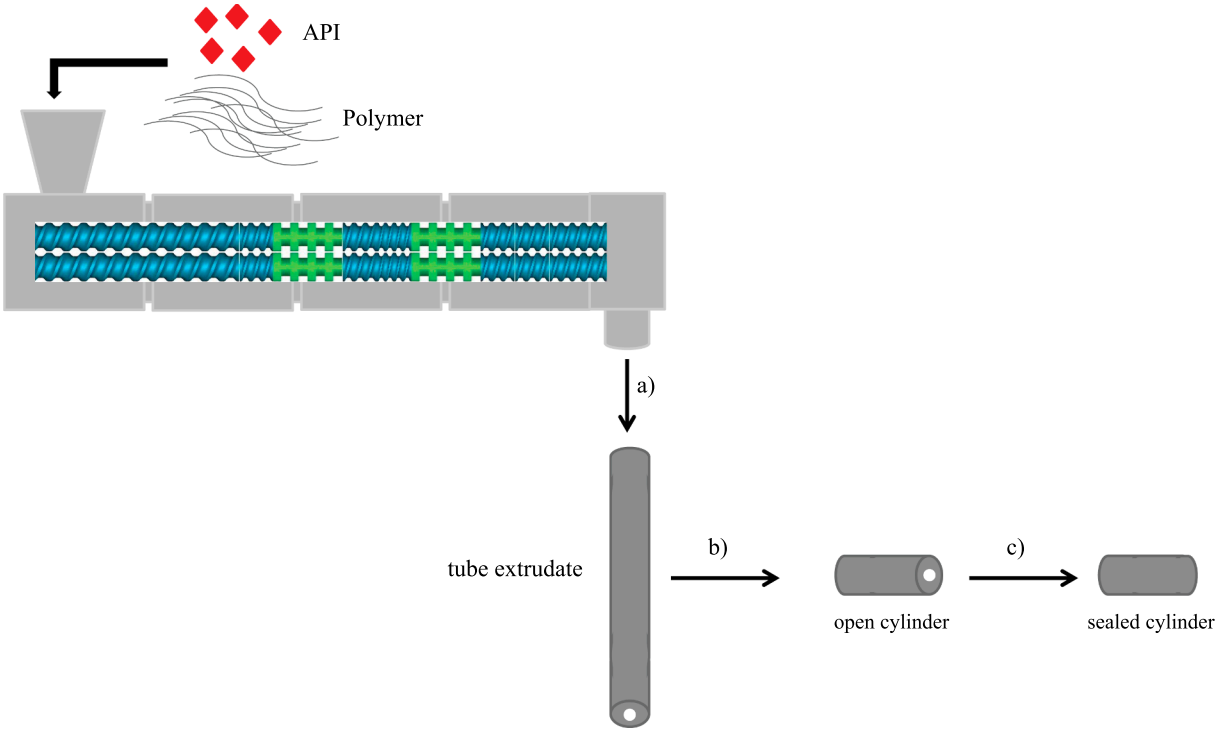

Fig. 1. Manufacturing process of hollow cylindrical extrudates. Process steps: (a) extrusion (b) cutting (c) sealing.

formulation drug load in order to achieve a final target dose of 300 mg. Finally, open cylinder ends were sealed using a heated circular cavity to obtain hollow bodies with an apparent density below 1 g/cm^3.

2.4. Design of the prolonged release profile

2.4.1. Formulation

The influence of various ratios of EuRS (pH independent, sustained release) and EPO (soluble < pH 5.0) on the release behavior of Met was investigated in combination with drug loads in the range of 50 – 80% (w/w).

2.4.2. Varying dimensions - wall thickness and surface area

The influence of varying OD/ID ratios on release profiles was examined. Therefore, extrudates based on two mixtures (Met 3 and Met 9, see Table 1) were prepared with (a) changing and (b) constant wall thicknesses. Tube extrudates were cut into 20 mm cylinders in length and sealed by closing the cavity on both sides with polyvinyl acetate, a water insoluble polymer. A temperature of about 90 °C was applied to soften the polymer. Hence, comparable hollow cylinder geometries were achieved to ensure accurate parameters for the investigated prediction models.

2.4.3. Variation of dose strength

Two batches (Met 3 and Met 9) were prepared as described in 2.3. To obtain hollow extrudates with different dose strength the length of the cylinders was varied. The influence of changing cylinder length on release behavior was evaluated. Extrudates containing 300, 400, 500 and 600 mg of Metformin per unit were produced.

2.5. True density

True densities (ρ_t) of *final blends* and unsealed tube cylinder extrudates were approximated using an AccuPyc 1330 helium pycnometer (Micromeritics GmbH, Norcross, USA; n = 1). Twenty purge cycles followed by 25 sample runs were performed to reach a standard deviation < 0.01%. Filling pressure and equilibration rate were kept constant for all experiments at 136.86 kPa·g and 0.0345 kPa·g/min respectively.

2.6. Apparent density

Apparent densities (ρ_a) of sealed extrudates were analyzed by displacement measurements using a GeoPyc 1360 (Micromeritics GmbH, Norcross, USA; n = 3). Blank measurements were performed constantly prior to sample analysis. Measurements were performed by running three cycles in a chamber (d = 12.7 mm) at a compression force of 28.0 N. Standard settings for zero depth (45.5427 mm) and conversion factor (0.1284 cm^3/mm) were applied.

2.7. Determination of extrudate dimensions

To measure outer (OD) and inner (ID) diameters, thin discs (< 2 mm; n = 4) of tube extrudates were cut precisely and photographed using a Canon EOS 700D camera (5184 × 3456 px) equipped with an EF-S 18–55 mm STM lens. The camera was fixed on a tripod to ensure a constant working distance for all images. Pictures were taken with a focal length of 55 mm and aperture priority mode. Pixel length corresponded to 13 µm. Cavity and total cross section areas were determined with NIH ImageJ [53,54]. OD and ID were calculated based on a disc circularity of one.

2.8. In vitro release studies

Release studies were performed using European Pharmacopoeia dissolution apparatus 1 (AT7smart; Sotax AG, Allschwil, Switzerland) with 500 ml of media kept at 37 °C +/− 0.5 °C and a stirring speed of 50 rpm. All experiments were conducted in triplicate. Samples were taken at predetermined time points over a 12 h period and analyzed online by a UV spectrophotometer (Agilent 8453; Agilent Technologies GmbH, Waldbronn, Germany). Metformin hydrochloride was detected at 245 nm using the first derivative of the absorbance. All experiments were conducted under sink conditions due to the high solubility of approximately 300 mg/ml of metformin hydrochloride in the pH range

of 1.2 – 6.8 [55]. Dissolution trials were carried out at three different pH levels using simulated gastric fluid (0.1 N HCl) pH 1.0 and McIlvaine buffer to obtain pH 4.0 and 6.0. In order to compare dissolution profiles, difference (f_1) and similarity (f_2) factors were calculated. Two dissolution curves are considered as equal if $f_1 \leq 15$ and $f_2 \geq 50$, respectively [56,57].

$$f_1 = \left(\frac{\sum_{t=t_1}^{t_n} |R_t - T_t|}{\sum_{t=t_1}^{t_n} R_t} \right) * 100 \quad (1)$$

$$f_2 = 50 * \log 10 \left[\frac{100}{\sqrt{1 + \frac{\sum_{t=t_1}^{t_n} (R_t - T_t)^2}{n}}} \right] \quad (2)$$

Mean dissolution values at time t of the reference product R_t and test product T_t as well as the sample number n are required for calculation.

2.9. Floating strength determination

In order to monitor the floating behavior continuously, an optimized quantitative floating force measurement system, based on the results reported by Timmermans and Moes was built [58]. A basket holder was directly mounted to the load cell of an Extend ED224S analytical balance (Sartorius AG, Göttingen, Germany). Thus, the resultant weight was measured in vertical direction (Fig. 2) without the need for calibrating the system prior to experiments. Resultant weight was recorded every 5 min over a period of 12 h using a custom made LabVIEW based software. Measurements were performed in 500 ml 0.1 N HCl with addition of 0.05% polysorbate 80, kept at 37 °C and stirred continuously, to create comparable conditions to *in vitro* release studies. The resultant floating force was calculated using the Archimedean principle Eq. (3),

$$F_{res} = F_{buoy} - F_{grav} \quad (3)$$

where the resultant force (F_{res}) is equal to the vector sum of the buoyancy (F_{buoy}) and gravity (F_{grav}) force. Tested extrudates are considered as "floatable" as soon as a force of zero mN/g is exceeded.

2.10. Scanning electron microscopy (SEM)

The matrix structure of hollow extrudates before and after drug release studies was examined at 10 kV and high vacuum conditions using an SU3500 SEM (Hitachi High-Technologies Europe GmbH; Krefeld, Germany) equipped with a SE-detector. Samples originating from dissolution studies were shock frozen in liquid nitrogen and subsequently freeze dried (Lyovac GT2, STERIS, Hürth, Germany) to preserve the pore structure. Samples were sputter coated with gold prior to SEM analysis.

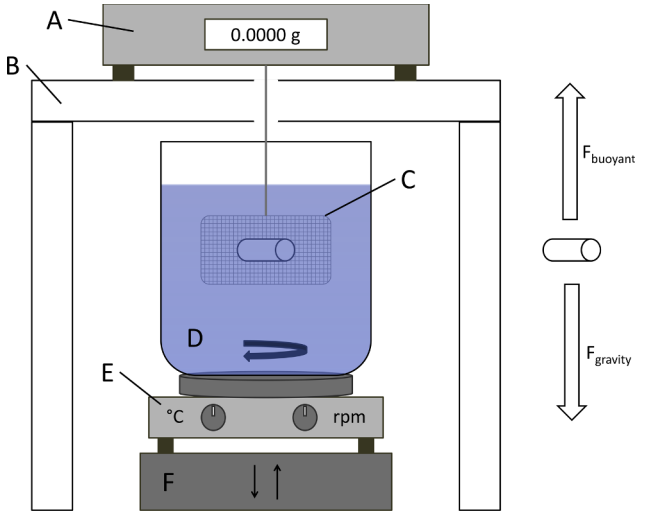

Fig. 2. Floating force measurement system. (A) Analytical balance, (B) table with a round recess, (C) basket, which is directly connected to the load cell, (D) glass vessel, (E) heated magnetic stir plate (F) lifting platform.

2.11. X-ray powder diffraction (XRPD)

Crystallinity was analyzed by X-ray powder diffraction. An X'Pert MRD Pro (PANalytical, Almelo, Netherlands) in reflection mode with Cu Kα1 radiation (45 kV/40 mA; λ = 1.5406 Å) was used. Measurements were performed with 0.0167° 2Θ step size in the range of 4.0–45.0° 2Θ. Extrudate samples were cryomilled prior to analysis. Data was analyzed with X'Pert High Score Plus (PANalytical, Almelo, Netherlands).

2.12. Non-linear curve fitting

Origin® Pro 8G (OriginLab, Northampton, USA) was used for mathematical description of dissolution profiles. Data was fitted based on the Weibull function (Eq. (4)),

$$C_t = C_0 \left(1 - e^{-\left(\frac{t}{k}\right)^d} \right) \quad (4)$$

where C_t and C_0 define the concentrations in solution at time t and after complete dissolution, d reflects the shape factor of the dissolution curve and k sets the time until 63.2% of the API is dissolved (rate constant). C_0 was set to 100 for all calculations. Data fitting was performed until no further changes in the function parameters were achieved (max. 400 iterations). In order to verify the quality of the performed fits, the adjusted correlation coefficients (R^2) were taken into consideration.

2.13. Predictive models

2.13.1. Die configuration for manufacture

The aim of the die configuration calculation is the determination of feasible OD to ID ratios, which can be used during manufacturing, in order to achieve an apparent density below 1 g/cm^3 of the final dosage form. Initially, the true density of the final powder blend (ρ_p) needs to be approximated using a helium pycnometer. Input parameters for the calculation are: drug load (dl) of the final blend, dose strength (ds) and desired density (ρ_d, < 1 g/cm^3) of the sealed final dosage form. For calculation, a zero porosity of the extrudate was assumed. In a first step the needed total volume (V_{tot}, including the hollow space) of the final dosage form to reach the desired density was calculated (Eq. (5)).

$$V_{tot} = \frac{\mathrm{ds}}{\mathrm{dl} * \rho_d} \quad (5)$$

In a second step, the required wall volume (V_{out}) to incorporate the polymer/Metformin mixture was defined (Eq. (6)),

$$V_{out} = \frac{ds}{dl * \rho_p} \quad (6)$$

followed by the cavity volume (V_{in}) determination (Eq. (7)).

$$V_{in} = V_{tot} - V_{out} \quad (7)$$

Based on the determined volumes, the calculation of possible OD/ID ratios to accomplish these volumes was carried out. The inner diameter has to be predefined due to the aforementioned available die parts. Subsequently the die parameter calculation was performed for all ID in order to choose the best possible die setting for manufacture, with preference on small overall dimensions to facilitate easy swallowing. Cylinder length (l) calculation (Eq. (8)) was based on the cavity volume. During the sealing process of the hollow cylinder, the volume of the

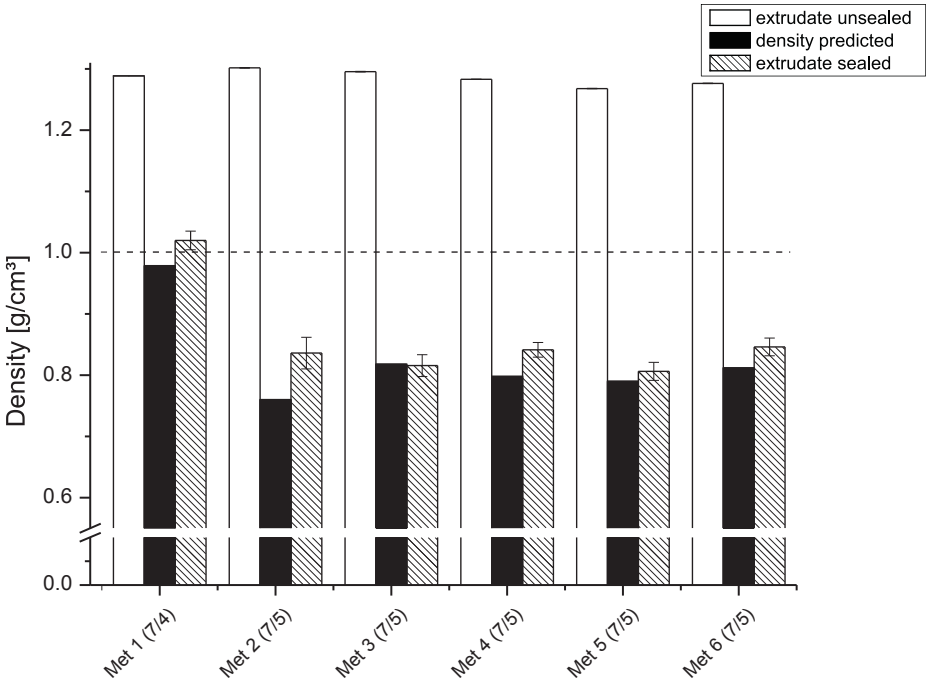

Fig. 3. Density comparison of unsealed extrudates (white bars; true density), predicted apparent density using Eq. (10), (11) of sealed extrudates (black bars) and measured apparent density of sealed extrudates (striped bars). Tested extrudates are considered "floatable" if the density is below 1 g/cm^3.

cavity was decreasing, whereas the total mass remained constant. Therefore, the total density increased. A correction factor (f_{cor}) was applied to counterbalance volume loss. The correction factor was determined empirically and varied between 1 and 2 mm for each side depending on the OD of the cylinder.

$$l = \frac{V_{in} * 4}{ID^2 * \pi} + 2 * f_{cor} \tag{8}$$

Taking cylinder length and ID into account, the outer diameter was calculated according to Eq. (9).

$$OD = \sqrt{\frac{V_{out} * 4}{l * \pi} + ID^2} \tag{9}$$

Calculated OD values usually deviated from the dimensions of the available die plates (6, 7, 8, 9 mm). Thus, a decision between the next smaller or larger diameter for implementation during manufacture must be made. In order to estimate the influence of diameter change on apparent density a predictive model was developed.

2.13.2. Apparent density

The two eligible ODs (next smaller and larger OD) yielded by the calculation of the die configuration were used to estimate the resulting apparent densities. Firstly, the resulting cylinder lengths of the two OD possibilities were calculated using the formula to determine the hollow cylinder volume, which was resolved to l (Eq. (10)). Secondly, the lengths obtained were individually inserted into Eq. (11)to calculate the corresponding apparent densities.

$$l = \frac{\frac{ds}{dl * \rho_p}}{\frac{\pi}{4} * (OD^2 - ID^2)} \tag{10}$$

$$\rho_{FDDS} = \frac{\frac{ds}{dl}}{\left(\frac{\pi}{4} * (OD^2 - ID^2) * l\right) + \left(\frac{\pi}{4} * ID^2\right) * (l - 2 * f_{cor})} \tag{11}$$

Based on the resulting densities, preferences for the smaller or larger diameter could be made. However, in case the smaller diameter exhibits a sufficiently low density (< 1 g/cm^3), it should be always preferred, as small sizes improve patient compliance.

2.13.3. Resultant floating force

The resultant force can be expressed according to the Archimedean principle (Eq. (3)). The buoyancy and gravity force can be described as follows,

$$F_{buoy} = \rho_s * \frac{m_{FDDS}}{\rho_{FDDS}} * g \tag{12}$$

$$F_{grav} = m_{FDDS} * g \tag{13}$$

where ρ_s is the solvent density, ρ_{FDDS} the apparent density and m_{FDDS} the mass of the dosage form. Insertion of Eqs. (12) and (13) into Eq. (3) yields the following expression.

$$F_{res} = \left(\rho_s * \frac{m_{FDDS}}{\rho_{FDDS}} - m_{FDDS}\right) * g \tag{14}$$

Input parameters were known (ρ_s, m_{FDDS}) or estimated based on the developed predictive models (ρ_{FDDS}), consequently the resulting floating force could be calculated prior to manufacture. Prediction was performed individually for each cylinder taking the actual mass into account. Subsequently, mean value and SD of three cylinders were calculated. In order to ensure comparability between different batches, the buoyancy force was normalized to the mass of the dosage form.

3. Results

3.1. Density prediction and die setting

The results of open and sealed extrudates density measurements as well as the predicted apparent densities of sealed extrudates are shown in Fig. 3. A comparison of measured values before and after sealing of samples manufactured with an outer to inner diameter ratio of 7/5 (Met 2 – 6) indicated, that a pronounced density reduction from approximate 1.28 g/cm^3 (unsealed extrudate) to 0.85 g/cm^3 (sealed extrudate) could be achieved. In contrast, sealed extrudates of sample Met 1 produced with a 7/4 OD/ID ratio could only reach a density slightly above 1 g/cm^3. Considering that Met 1 and Met 2 consist of identical mixture

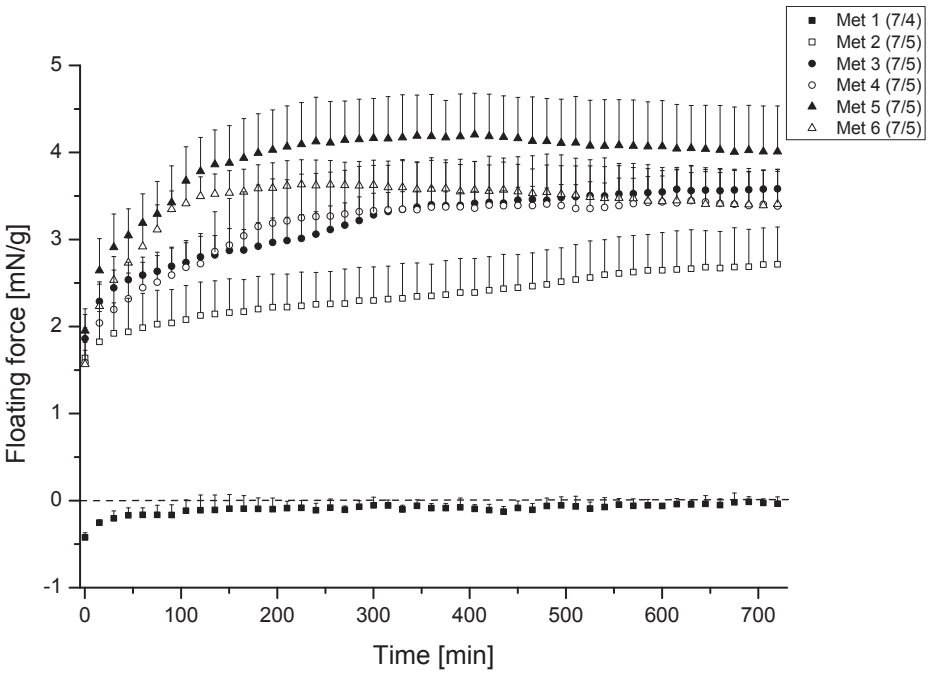

Fig. 4. Floating behavior of formulation Met 1 – 6 was performed in triplicate in 500 ml 0.1 N HCL with addition of 0.05% polysorbate 80 at 37 ± 0.5 °C. To increase the readability, every third measured value is shown and SD are displayed only in positive direction (negative SD have the same value).

compositions and differ only in the OD/ID ratio, the major impact of a varying cavity volume on the density becomes apparent. Predicted values were plotted against the measured densities (Fig. 3), in order to assess the prediction quality. With the exception of a slightly larger deviation for batch Met 2, the prediction model could reproduce the measured sealed densities with a good accordance.

3.2. Buoyancy measurements

Experiments assessing the ability of the gastroretentive dosage form to stay buoyant in simulated gastric fluid (Fig. 4) showed an immediate floatability of Met 2 – 6, which were manufactured with an 7/5 OD/ID ratio. The dosage forms stayed buoyant for the whole 12 h measuring period. Moreover, buoyancy did not decrease over time, but instead increased in particular within the first three hours. In contrast, extrudates of Met 1 could not achieve a positive floating force ($F_{buoy} < F_{grav}$) and were thus not able to float in gastric fluid. Using Eq. (14), the buoyant force was estimated based on the apparent density and mass of the dosage form. Fig. 5 illustrates predicted values (red stars) plotted against measured buoyancy values (striped bars) at the time of 5 min. Calculated mean values (n = 3) were within the standard deviation of the measured samples for all floating formulations. Up- and downward tendencies of the buoyancy force could be depicted precisely using the predictive model.

3.3. In vitro dissolution studies

3.3.1. pH 1.0

The influence of different ratios of the freely miscible polymers EuRS (pH independent, sustained release) and EPO (soluble < pH 5.0) on the release behavior of Met was investigated as shown in Fig. 6. With increasing amounts of EPO accelerated release kinetics were observed. Nevertheless, a sustained release profile could be achieved for all formulations, even for the highest drug load of 80% (w/w, Met 10). Despite the very high drug loading, no burst release was detected for any sample. An increase in drug loading from 70% to 80% (Met 2 and 10) led to a much faster release. Comparing the release patterns of Met 1 and Met 2, which differ only in the ID/OD ratio (7/4 vs. 7/5), Met 1 exhibited a slower release profile.

3.3.2. Elevated pH conditions

Stomach pH values can vary over a wide range. Therefore, dissolution test at elevated pH conditions (pH 4 and 6) were conducted in order to examine the pH sensitivity of the formulation. From the data in Fig. 7A and B, it is apparent that a change from pH 1 to pH 4 (dashed lines) had only minor effects on the release properties of tested formulations. Calculated f values shown in Table 2 also confirmed that the dissolution curves at pH 1 and 4 could be regarded as equivalent, since $f_1 < 4$ and $f_2 > 78$ represented a high similarity. In contrast, at pH 6 (dotted lines), all investigated formulations were considerably influenced hence resulting in a decreased dissolution rate. Calculated f values consequently exceeded the similarity limits. Moreover, the sensitivity to pH changes was more pronounced for extrudates containing a high amount of EPO.

3.3.3. Variation of dose strength and extrudate dimensions

Fig. 8A revealed that varying the cylinder length had almost no impact on the release properties of tested samples. Calculated f_1 and f_2 values (data not shown) confirmed a high similarity of the release curves. The buoyancy was maintained for 12 h for all samples. However, the change in wall thickness had a strong influence on the rate of release. Fig. 8B demonstrated that with increasing thickness, the release rate declined. For Met 9, the release after 6 h decreased from 97.7% for a OD/ID ratio of 7/5 to 73.6% for 7/4 and down to 64.4% for 7/3. At the same time the surface mass ratio (Table 3) decreased from 8.7 to 5.4 cm^2/g with an increasing wall thickness (7/5 → 7/3). This tendency could be shown for both investigated batches, confirming the trend already observed for formulations Met 1 and 2 (Fig. 6).

In vitro release profiles of extrudates with varying OD while maintaining the wall thickness constant are shown in Fig. 8C. Graphs of Met 9 are almost completely superimposed, except in the last 3 h, while the ones of Met 3 show a slight offset. Taking the mass normalized areas into account (Table 3), it is striking that these are almost completely identical for Met 9 (6.12 ± 0.25; 6.16 ± 0.21; 6.20 ± 0.22), but differ slightly for Met 3 (7.03 ± 0.02; 6.67 ± 0.09; 6.37 ± 0.06). Weibull fitting was performed for both batches. The mainly recipe-

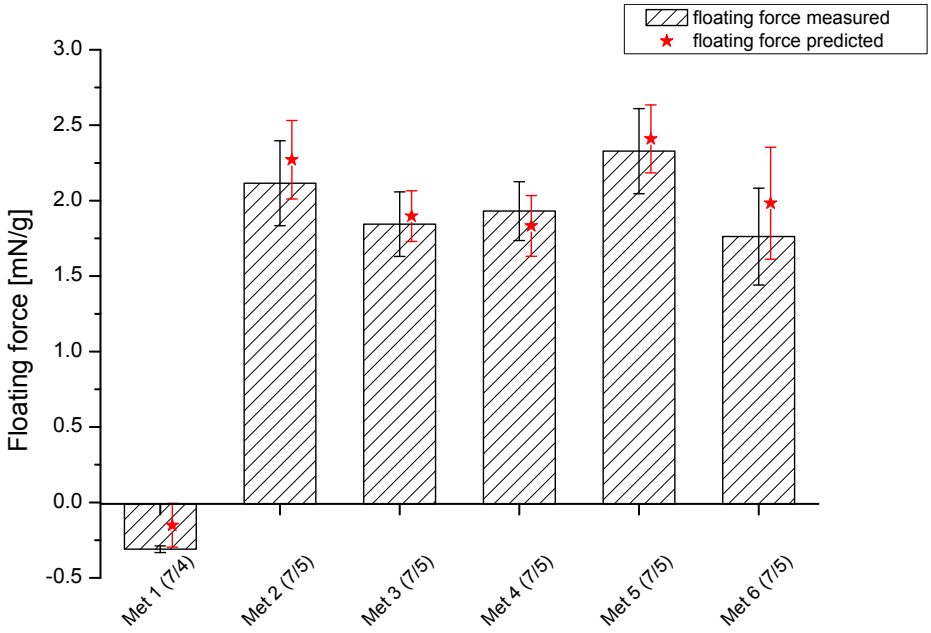

Fig. 5. Predicted floating forces (red stars) compared with measured buoyancy values (striped bars). Experiments and calculations were done in triplicate; mean values ± SD are shown. (For interpretation of the references to colour in this figure legend, the reader is referred to the web version of this article.)

dependent value *d* could be kept approximately constant (Met 3: 0.567 ± 0.051; Met 9: 0.793 ± 0.053) for the respective mixture. In contrast, the calculated velocity value *k* (Table 3) displayed a strong dependency on wall thicknesses. The linear relationship of *k* and the surface volume ratio of the matrix found by Kosmidis et al. could not be confirmed in our experiments [59,60]. However, a good correlation was achieved by plotting the mass normalized surface against ln k (Fig. 8D).

3.4. SEM

To investigate the extrudate morphology, SEM images of Met 3 were taken before and after 12 h dissolution (Fig. 9A–D). The extrudate surface prior to release (B) has a slightly rough but very dense structure confirming the appropriateness of zero porosity assumption for our prediction models. The cross section image of the cylinder (D) highlights the completely non-porous wall structure. After release (A and C) several pores are visible on the surface area as well as a porous, sponge-like structure in the cross section image. The emerging porosity in the cylinder wall did not influence floatability as the remaining pores were filled with water, trapping the air inside. Cylinder wall properties before and after dissolution differ with regard to mechanical strength. Hardness before dissolution tested at right angle to the cylinder length was above 100 N for all investigated samples. As the dissolution time progressed, the cylinders softened due to water uptake and the release

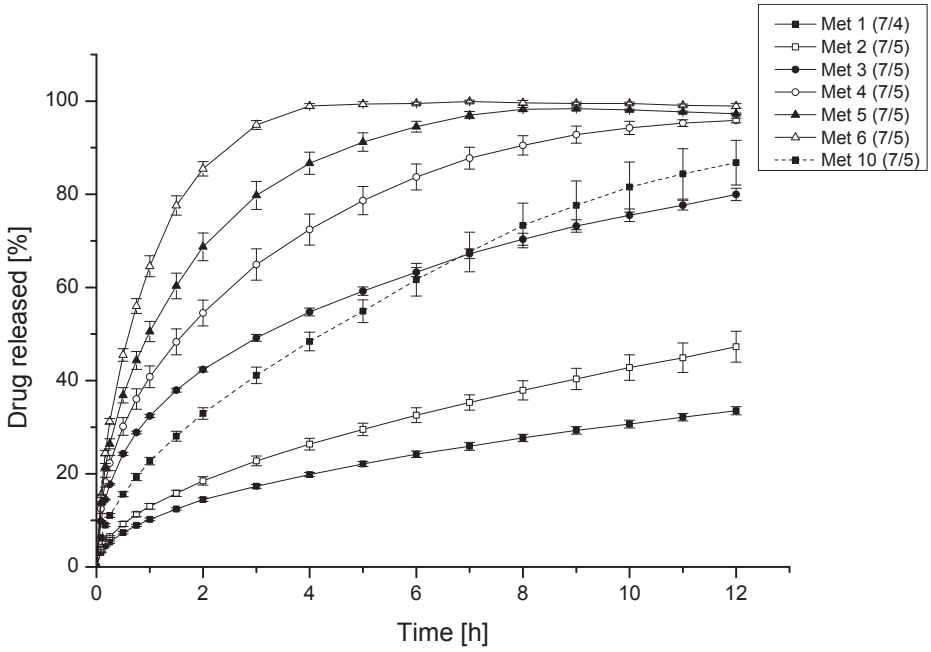

Fig. 6. Effect of different EuRS/EPO ratios on dug release of 300 mg sealed floating extrudates (Met 1 – 6). Trials were performed in 500 ml 0.1 N HCL at 37 ± 0.5 °C (50 rpm, Eur. Ph. Apparatus 1). Mean value ± SD (n = 3).

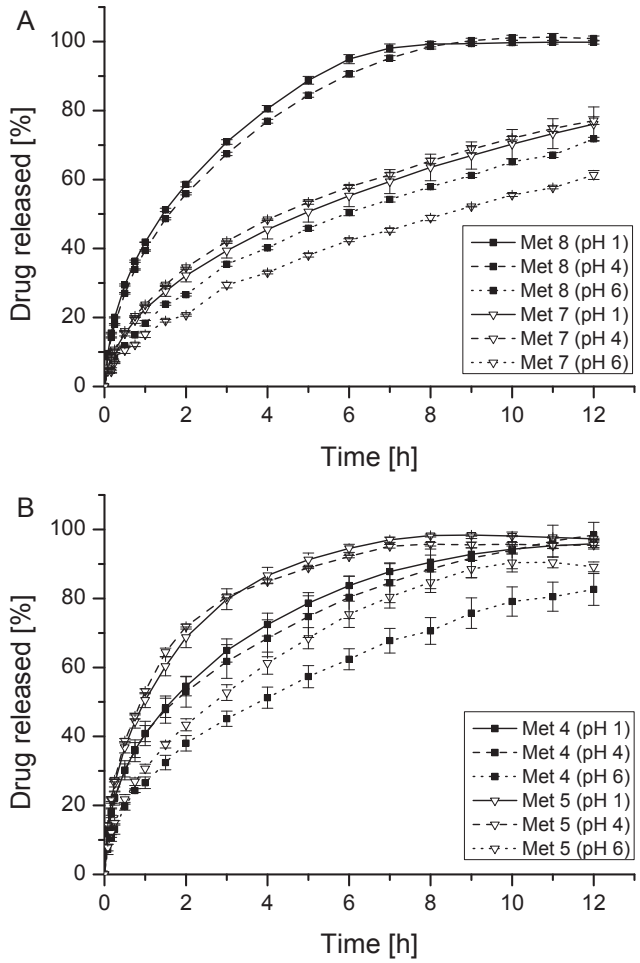

Fig. 7. A-B Effect of pH changes on release properties of 300 mg samples of (A) Met 7 and 8 (50% DL, 7/4), (B) Met 4 and 5 (70% DL, 7/5). Trials were performed in 500 ml 0.1 N HCl (pH 1.0 - solid line) or rather McIlvaine buffer (pH 4 – dashed line, pH 6 – dotted line) at 37 ± 0.5 °C (50 rpm, Eur. Ph. Apparatus 1). Mean value ± SD (n = 3).

Table 2
Calculated f_1 and f_1 values for *in vitro* release of metformin at pH 4 and 6 taking pH 1 as reference sample.

sample	pH	f_1	f_2
Met 4	4.0	2.55	81.63
	6.0	24.55	39.75
Met 5	4.0	2.87	80.81
	6.0	22.57	38.17
Met 7	4.0	3.99	84.00
	6.0	24.81	47.48
Met 8	4.0	3.41	78.30
	6.0	44.50	24.86

of Metformin and EPO from the matrix.

4. Discussion

The apparent density is an important criterion for the development of FDDS as it allows a direct statement about the buoyancy of the system. The large density drop for samples Met 2 – 6 to approximately 0.85 g/cm^3 (see Fig. 3) clearly highlights that the cavity volume was sufficient to ensure floatability on gastric fluids. Comparing Met 1 and 2, which differ only in the inner diameter, it is obvious that the ratio between inside and outside diameter has a significant influence on the final density. Predicted density values were in good accordance to the measured values of sealed extrudates confirming that the calculation allows a reasonable prediction. The slightly larger deviation of measured and predicted values for Met 2 are likely caused by cavity variations due to manually cutting and sealing of each individual dosage form. Comparing the apparent density and floating force results (Figs. 3 and 4) a direct correlation could be established. Since buoyant force depends mainly on the dosage form density, which can easily be measured, calculations were carried out to estimate the floating force (Eq. (14)). Predicted values for the 5 min time point (see Fig. 5) were in good accordance with the measured floating force values, demonstrating that the prediction could be conducted with sufficient accuracy.

Fig. 4 illustrates, that all samples manufactured with a 7/5 diameter ratio, which had a density less than 1 g/cm^3, float immediately, thereby reducing the risk of premature gastric emptying. Sample Met 1 was unable to float as the buoyancy force was insufficient, which was consistent with previously shown density results. Floating cylinders showed buoyancy forces in the range of 2 – 4 mN (corresponds to 200 – 400 mg) which are comparable with formulations developed by Vo et al. and Timmermans et al. which were in a range of 1 – 5 mN [43,58]. Eisenächer et al. investigated the influence of a viscosity change (300 mPa * s) of the gastric fluid (i.e. meal intake) on the buoyancy force (< 400 mg) of coated tablets. Floating strength was decreased by 15% without effecting the floatability and duration [27]. Since the buoyancy force is comparable to our samples, the developed hollow cylinders should float in viscous fluids, respectively. Fortunately, the floating force did not decrease over time as reported in various studies [27,43], but instead increased especially during the first three hours. SEM images (see Fig. 9) indicate that even after 12 h dissolution, the matrix scaffold of Eudragit® RS remained intact whereas the API diffused from the polymer matrix. It was concluded that drug diffusion provokes a mass loss while the cylinder dimensions remain constant. Consequently, the apparent density of the dosage form decreases, resulting in an increase in floating force. As the buoyancy force shows an increasing tendency, the predicted floating force value can be considered as the minimum floating force. The ratio of OD/ID diameter was identified as a critical parameter for buoyancy and should therefore be closely monitored during manufacture. The possibility to predict the apparent density and subsequently the floating force prior to manufacture is a considerable advantage of the novel tube extrusion approach. The number of experiments can be significantly reduced as the calculation of the final density can be used to select an optimal die setting (i.e. OD/ID ratio) in order to ensure buoyancy. *In vitro,* the floating cylinders showed very promising buoyancy properties. However, retaining the delivery system in the stomach represents a major challenge especially in the fasted state. Very small liquid amounts (< 50 ml) and strong propulsive contractions towards the pylorus could lead to a rapid gastric transit of a floating dosage form [1]. The fact that the hollow cylinders were directly floatable could be advantageous compared to systems that generate their buoyancy in situ (e.g. gas generating systems), thereby avoiding fast gastric transit. Nonetheless, gastro retention at fasted conditions seems to be challenging in general [61,62]. The retention time of gastroretentive floating systems is strongly depending on meal ingestion [63]. Food intake leads to the interruption of the migration motor complex and a constriction of the pylorus, increasing the likelihood of retention of monolithic systems in the stomach [64]. Studies comparing FDDS with non-floating systems after a meal intake demonstrated a prolonged retention time of the FDDS in the stomach. This confirms that the floating approach can prevent premature gastric emptying [24,65,66]. Beside meal intake, the body position has an important impact on the success of a FDDS. Gastric emptying and also the antral mixing properties change by varying the body position [67,68]. Moreover, a floating of the dosage form towards the pylorus could be possible, which may cause a fast stomach transit. To clarify the influence of described physiological factors on the gastroretentive properties of the developed floating cylinders, *in-vivo*

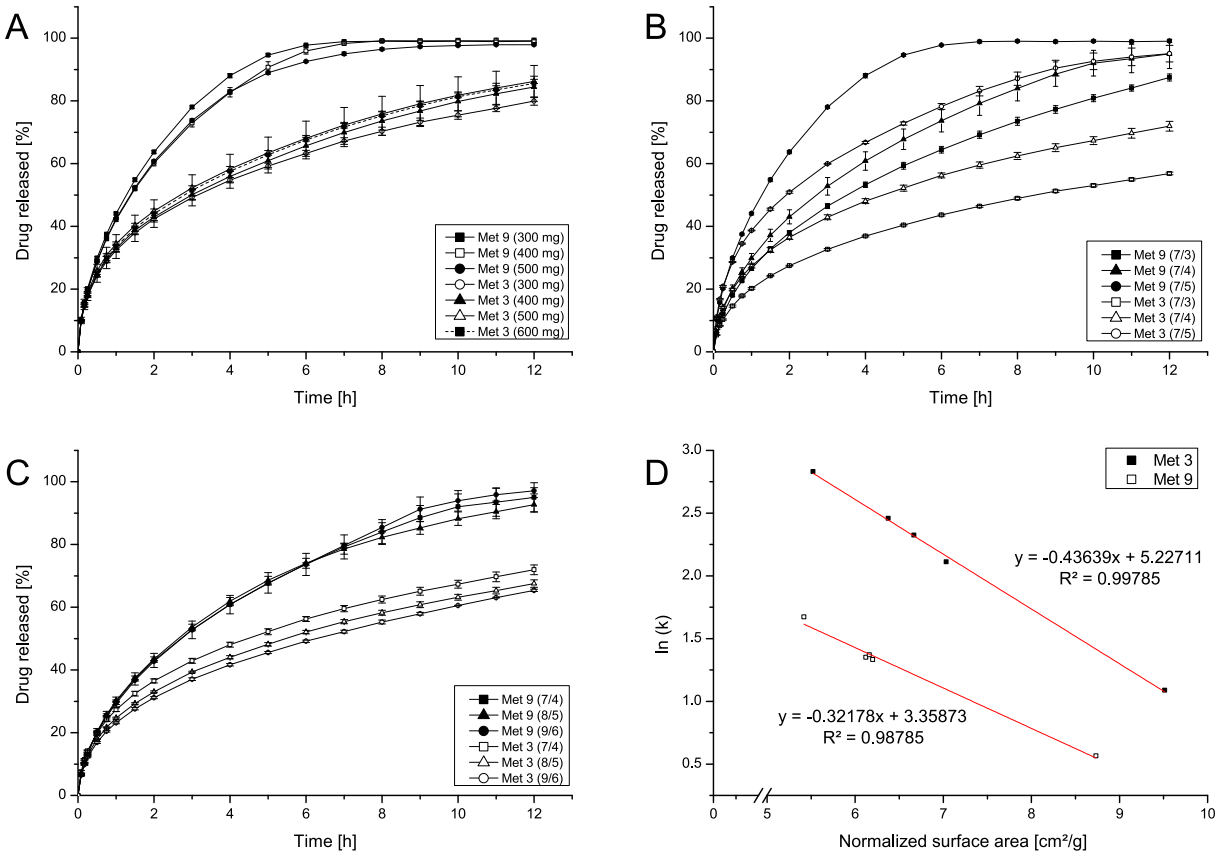

Fig. 8. A-D Influence of extrudate dimensions on the on release properties of metformin formulations conducted in 500 ml 0.1 N HCL at 37 ± 0.5 °C (50 rpm, Eur. Ph. Apparatus 1). Mean value ± SD (n = 3). Variation of (A) cylinder length (dose variation 300 mg – 600 mg) (B) wall thickness and (C) surface area. Correlation between normalized surface area and ln *k* (Weibull) (D). Detailed information about dimensions and surface areas are listed in Table 3.

studies need to be conducted in which the performance in fasted and fed state are examined, ideally taking different body positions into account.

A wide range of sustained release profiles with drug loads up to 80% were achieved (Fig. 6) using various mixtures of Eudragit® RS and EPO. The release rate can be precisely controlled by the ratio of the two polymers. Increasing the proportion of Eudragit® E led to accelerated release profiles. Despite the very high drug loading, no burst release was detected for any sample. Dissolution profiles of Met 10 (80% drug load) varied more compared to other formulations investigated. Homogeneous drug release requires a homogeneous distribution of matrix polymer throughout the matrix, i.e. a percolating network of polymer matrix [69]. However, according to Leuenberger et al. 80% of drug load is likely to be close or even below the percolation threshold [70]. The subsequent inhomogeneous polymer distribution would thus explain the observed higher variance in drug release. Taking the SEM images into account, the decreasing release rate over time of each profile can be explained by an extended diffusion path of the API, confirming a diffusion controlled matrix release mechanism (see suppl. data Table A.1). Samples manufactured with a diameter ratio of 7/5 were able to float directly and for the duration of 12 h on simulated gastric fluid. Figs. 4 and 6 confirmed the possibility to vary the cylinder wall composition, i.e. active ingredient and polymer, without considerably changing the buoyancy of the system. Due to the hollow cylinder design buoyancy was almost exclusively dependent on the OD/ID ratio and not on the polymer properties. In contrast to the previous approaches of other researchers, the polymer has no double function, i.e. ensure floating ability and control of the drug release [28,34]. By

Table 3
Properties of extrudates investigated by changing ratios of OD to ID diameter. Weibull function (Eq. (4)) was used to determine the rate constant *k* and shape factor *d* of the corresponding release profile.

Sample	ID [mm] ± SD	OD [mm] ± SD	Cylinder surface area [mm²] ± SD	Mass normalized surface area [cm²/g] ± SD	Rate constant *k* ± SE	Shape factor d ± SD
Met 9 (7/3)	2.71 ± 0.03	7.15 ± 0.02	444.18 ± 13.22	5.42 ± 0.22	5.338 ± 0.14	
Met 9 (7/4)	3.59 ± 0.06	7.09 ± 0.04	451.57 ± 12.82	6.12 ± 0.25	3.863 ± 0.098	
Met 9 (7/5)	4.67 ± 0.08	7.02 ± 0.03	444.04 ± 5.06	8.73 ± 0.04	1.767 ± 0.051	0.793 ± 0.053
Met 9 (8/5)	4.59 ± 0.06	7.99 ± 0.04	506.99 ± 9.17	6.16 ± 0.21	3.942 ± 0.115	
Met 9 (9/6)	5.60 ± 0.06	9.07 ± 0.04	572.80 ± 15.89	6.20 ± 0.22	3.790 ± 0.105	
Met 3 (7/3)	2.92 ± 0.03	6.86 ± 0.02	433.81 ± 6.69	5.52 ± 0.12	16.968 ± 0.742	
Met 3 (7/4)	3.82 ± 0.08	7.05 ± 0.04	450.22 ± 2.74	7.03 ± 0.02	8.265 ± 0.219	
Met 3 (7/5)	4.72 ± 0.03	6.98 ± 0.04	444.59 ± 2.42	9.51 ± 0.09	2.971 ± 0.061	0.567 ± 0.051
Met 3 (8/5)	4.69 ± 0.02	7.81 ± 0.03	495.01 ± 3.61	6.67 ± 0.09	10.220 ± 0.126	
Met 3 (9/6)	5.69 ± 0.03	8.82 ± 0.03	564.32 ± 1.05	6.37 ± 0.06	11.690 ± 0.157	

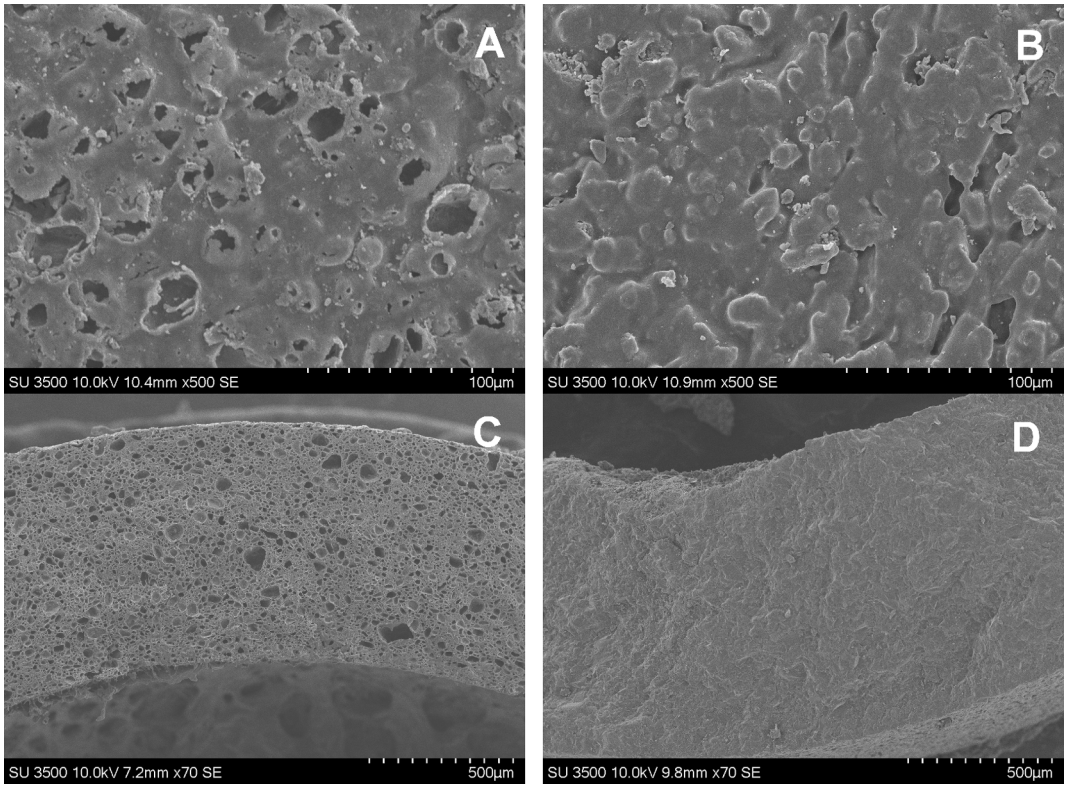

Fig. 9. A–D Representative SEM images of extrudate morphologies prior (B and D) and after (A and C) 12 h dissolution prepared from formulation Met 3 (7/5). Images A and B represent the cylinder surface area captured with a 500x magnification, whereas C and D show cross sections (70x magnification) of the cylinder wall.

separation of floatability and release control, hollow tube shaped extrudates allowed various possibilities during formulation development with regards to the achievement of tailored dissolution profiles. However, a certain quantity of sustained release polymer (> 7% of EuRS) was mandatory to form a coherent matrix structure. Otherwise, the integrity of the FDDS capsule could not be guaranteed. Since EuRS is a non-degradable polymer, one could argue that there is a potential risk that the FDDS could accumulate in the stomach. During dissolution studies a softening of the cylinders due to water uptake and diffusion of Metformin and EPO out of the matrix was observed. The degree of softening increased with decreasing proportion of EuRS in the matrix. Due to gastric motility, softening will increase the likelihood of cylinder collapse, resulting in a loss of buoyancy. As softening progressed with drug release, the systems would hence support a controlled exit from the stomach. Of course, this hypothesis needs to be confirmed *in-vivo*.

A varied wall thickness influenced not only the buoyancy but also the release behavior. As can be seen in Fig. 6, Met 1 (7/4) showed a slower rate of release compared to Met 2 (7/5). In order to evaluate the influence of wall thickness and cylinder surface area on API release properties, samples with varying dimensions were investigated. A pronounced decrease in dissolution rates with increasing wall thickness was observed (Fig. 8B) pointing out the importance of the ID/OD ratio for the release properties. Increased wall thickness resulted in extended diffusion paths, thereby decreasing the release rate. A study published by Maus et al., where the effect of geometry on drug release using hot-melt extruded sustained release pellets was investigated, showed that drug release is mainly governed by the area/volume ratio [71]. Similar observations could be made for the area/mass ratio in the current study. The surface area remained constant since there was no change in external diameter. However, the mass normalized surface area decreased with an increasing wall thickness leading to a slower drug release. In contrast, samples with constant wall thickness but varying external diameters showed almost identical dissolution profiles. This finding was in accordance with the aforementioned matrix-mediated release since unchanged wall thicknesses resulted in identical diffusion paths. This illustrates that the diameter of the hollow cylinders may be varied without affecting the release kinetics as long as the wall thickness is kept constant. Nevertheless, taking into account the cylinder surface areas, which rose with increasing external diameter, an accelerated release rate could also be expected. Surprisingly, the 7/4 sample of Met 3 showed the fastest release although it had the smallest surface area (Table 3). However, calculated mass normalized areas exhibited a reduced tendency with increasing external diameter for Met 3 samples. Based on this observation one could conclude that Met 3 sample 7/4 would have a faster release compared to sample 9/6, which was in accordance with the results in this study. Regarding Met 9 samples, mass normalized surface areas remained nearly unchanged, consistent with the superimposed dissolution profiles. Consequently, the surface/mass ratio was identified as the discriminating factor on release properties. The rate constant k (Weibull fit) of respective samples was calculated (Eq. (4)) and plotted against the surface/mass ratio (Fig. 8D). A linear relationship between both parameters with acceptable correlation coefficients of 0.99785 and 0.98785 was found. The obtained correlation enabled the estimate of release profile shifts caused by changes of geometric proportions. Furthermore, release profiles could be controlled by varying the ID/OD ratio. However, the change in diameter ratio is only possible up to the geometric limitations defined by enabling floatability.

By varying the cylinder length, dose strength could be doubled without considerably affecting the release profile (Fig. 8A). Conducted f_1 and f_2 tests confirmed the high similarity. Due to the hollow tube shape, a change in length did not lead to a change in diffusion pathways. In addition, a change of the surface/mass ratio did not occur. Since both factors that mainly influenced the release behavior remained constant, a change in dissolution rate was neither expected nor observed. Furthermore, higher dose strength was achieved without affecting release properties by increasing the outer diameter while keeping the wall thickness constant. By combining both concepts, the

dose could be varied over a wide range, limited only by the overall dimensions to enable easy swallowing. The dimensions should be kept as small as possible to ensure a good application. Samples manufactured with a 7 mm OD are comparable in size to a standard zero capsule. Due to the smooth surface of the extrudates an easy swallowing is likely. Additionally, a non-functional coating to improve the applicability would be conceivable. With regards to formulation development, the ability to change the dose without affecting the release rate is highly beneficial as it would not be necessary to adjust the formulation composition for each dose level.

Aside from the controllable variables such as extrudate dimensions and matrix composition, the drug release strongly depended on the stomach pH value. Depending on meal or intake of medication e.g. proton pump inhibitors, stomach pH levels can vary over a wide range (1.4 – 5.4; peak value 6.7) [72,73]. As EPO is soluble up to pH 5, experiments were conducted above and below the solubility limit in order to evaluate the robustness of the formulation. Due to the pH independent controlled release behavior of EuRS, observed changes in dissolution were mainly attributed to EPO. Exceeding the dissolution pH of EPO resulted in a slower release rate for all batches. The effect was most pronounced for sample Met 8, which contained the highest fraction of EPO. Based on the fact that EPO could no longer dissolve but instead was rather forming a gel, the formation of pores was obstructed and a slower rate of drug diffusion from the polymer matrix resulted. In order to increase the pH robustness, a polymer exchange would be conceivable, e.g. against a soluble grade of polyvinylpyrrolidone. To evaluate the influence of solid state changes e.g. amorphisation on release behavior, XRPD experiments were performed. No changes in crystallinity after extrusion were detected. Therefore, effects on dissolution behavior due to solid state changes could be excluded. Exemplary figures are listed in the supplementary data. The presented system displayed *in vitro* superior properties compared to other floating devices, which will be investigated *in vivo* in a future study.

5. Conclusion

In the present study, tube extrusion was successfully used to prepare hollow floating drug delivery systems in only three process steps, i.e. extrusion, cutting and sealing. A sustained release over 12 h in combination with a drug load of up to 80% without any burst release was achieved. It was shown that apparent density and resulting buoyancy force could be predicted accurately prior to extrusion. Wall thickness and surface/mass ratio were identified to be the main geometric factors influencing the release properties. Consequently, by monitoring the ID/OD ratio during manufacture, both the buoyancy and the release of the dosage form could be precisely controlled. A big advantage of the novel approach is the possibility to vary the release profile of the system without essentially affecting the buoyancy. Moreover, the diffusion matrix-controlled release allows for the dose of the active ingredient to be varied without affecting its release profile, as long as maintaining the geometric ratios of the hollow cylinder. For investigated mixtures, the 7/5 diameter ratio has shown to be the optimum for achieving sufficient buoyancy while maintaining the cylinder dimensions as small as possible. The manufacture of extrudates with 80% drug load, leading to very small dosage units was possible. Nevertheless cylinders with 70% drug load should be preferred since they provided higher flexibility in terms of release control. The selection of the release profile is dependent on the target dose regimen and pharmacokinetic parameters, e.g. half-life of the active ingredient. Based on the opportunity of precise release control, the profiles can be tailored to the specific demands. In conclusion, the number of experiments required to achieve a buoyant system with desired release properties can be reduced due to the high flexibility and good predictability of this new approach.

Acknowledgement

The authors would like to thank Prof. Dr. P. Kleinebudde and his research group from the institute of Pharmaceutics and Biopharmaceutics at the University of Düsseldorf for the opportunity to use the Geopyk 1360 for density measurements. We also would like to thank Alexander Denninger for software support on LabView. This research did not receive any specific grant from funding agencies in the public, commercial, or not-for-profit sectors.

Appendix A. Supplementary material

Supplementary data to this article can be found online at https://doi.org/10.1016/j.ejpb.2019.02.022.

References

[1] M. Grimm, M. Koziolek, J.-P. Kühn, W. Weitschies, Interindividual and intraindividual variability of fasted state gastric fluid volume and gastric emptying of water, Eur. J. Pharm. Biopharm. 127 (2018) 309–317, https://doi.org/10.1016/j.ejpb.2018.03.002.
[2] A. Steingoetter, M. Fox, R. Treier, D. Weishaupt, B. Marincek, P. Boesiger, M. Fried, W. Schwizer, Effects of posture on the physiology of gastric emptying: a magnetic resonance imaging study, Scand. J. Gastroenterol. 41 (2006) 1155–1164, https://doi.org/10.1080/00365520600610451.
[3] J. Fidler, A.E. Bharucha, M. Camilleri, J. Camp, D. Burton, R. Grimm, S.J. Riederer, R.A. Robb, A.R. Zinsmeister, Application of magnetic resonance imaging to measure fasting and postprandial volumes in humans, Neurogastroenterol. Motility 21 (2009) 42–51, https://doi.org/10.1111/j.1365-2982.2008.01194.x.
[4] D.M. Mudie, G.L. Amidon, G.E. Amidon, Physiological parameters for oral delivery and *in Vitro* testing, Mol. Pharm. 7 (2010) 1388–1405, https://doi.org/10.1021/mp100149j.
[5] J.B. Dressman, R.R. Berardi, L.C. Dermentzoglou, T.L. Russell, S.P. Schmaltz, J.L. Barnett, K.M. Jarvenpaa, Upper gastrointestinal (GI) pH in young, healthy men and women, Pharm. Res. 7 (1990) 756–761.
[6] F. Schneider, M. Grimm, M. Koziolek, C. Modeß, A. Dokter, T. Roustom, W. Siegmund, W. Weitschies, Resolving the physiological conditions in bioavailability and bioequivalence studies: comparison of fasted and fed state, Eur. J. Pharm. Biopharm. 108 (2016) 214–219, https://doi.org/10.1016/j.ejpb.2016.09.009.
[7] J. Van Den Abeele, J. Rubbens, J. Brouwers, P. Augustijns, The dynamic gastric environment and its impact on drug and formulation behaviour, Eur. J. Pharm. Sci. 96 (2017) 207–231, https://doi.org/10.1016/j.ejps.2016.08.060.
[8] E.A. Klausner, S. Eyal, E. Lavy, M. Friedman, A. Hoffman, Novel levodopa gastroretentive dosage form: in-vivo evaluation in dogs, J. Control. Release 88 (2003) 117–126.
[9] N.C. Ngwuluka, Y.E. Choonara, G. Modi, L.C. du Toit, P. Kumar, V.M.K. Ndesendo, V. Pillay, Design of an interpolyelectrolyte gastroretentive matrix for the site-specific zero-order delivery of levodopa in Parkinson's disease, AAPS PharmSciTech. 14 (2013) 605–619, https://doi.org/10.1208/s12249-013-9945-1.
[10] C. Chen, V.E. Cowles, M. Sweeney, The intestinal absorption mechanism of gabapentin makes it appropriate for gastroretentive delivery, Curr. Clin. Pharmacol. 8 (2013) 67–72, https://doi.org/10.2174/1574884711308010009.
[11] B.E. Gidal, J. DeCerce, H.N. Bockbrader, J. Gonzalez, S. Kruger, M.E. Pitterle, P. Rutecki, R.E. Ramsay, Gabapentin bioavailability: effect of dose and frequency of administration in adult patients with epilepsy, Epilepsy Res. 31 (1998) 91–99.
[12] L.Z. Benet, Pharmacokinetics/pharmacodynamics of furosemide in man: a review, J. Pharmacokinet. Biopharm. 7 (1979) 1–27, https://doi.org/10.1007/BF01059438.
[13] L. Meka, B. Kesavan, V.N. Kalamata, C.M. Eaga, S. Bandari, V. Vobalaboina, M.R. Yamsani, Design and evaluation of polymeric coated minitablets as multiple unit gastroretentive floating drug delivery systems for furosemide, J. Pharm. Sci. 98 (2009) 2122–2132, https://doi.org/10.1002/jps.21562.
[14] P.L. Bardonnet, V. Faivre, W.J. Pugh, J.C. Piffaretti, F. Falson, Gastroretentive dosage forms: overview and special case of Helicobacter pylori, J. Control. Release 111 (2006) 1–18, https://doi.org/10.1016/j.jconrel.2005.10.031.
[15] P.S. Rajinikanth, J. Balasubramaniam, B. Mishra, Development and evaluation of a novel floating in situ gelling system of amoxicillin for eradication of Helicobacter pylori, Int. J. Pharm. 335 (2007) 114–122, https://doi.org/10.1016/j.ijpharm.2006.11.008.
[16] L. Kagan, N. Lapidot, M. Afargan, D. Kirmayer, E. Moor, Y. Mardor, M. Friedman, A. Hoffman, Gastroretentive accordion pill: enhancement of riboflavin bioavailability in humans, J. Control. Release 113 (2006) 208–215, https://doi.org/10.1016/j.jconrel.2006.03.022.
[17] L. Yin, C. Qin, K. Chen, C. Zhu, H. Cao, J. Zhou, W. He, Q. Zhang, Gastro-floating tablets of cephalexin: preparation and in vitro/in vivo evaluation, Int. J. Pharm. 452 (2013) 241–248, https://doi.org/10.1016/j.ijpharm.2013.05.011.
[18] E.A. Klausner, E. Lavy, D. Stepensky, E. Cserepes, M. Barta, M. Friedman, A. Hoffman, Furosemide pharmacokinetics and pharmacodynamics following gastroretentive dosage form administration to healthy volunteers, J. Clin. Pharmacol.

43 (2003) 711–720, https://doi.org/10.1177/00912700003254575.
[19] G. Gusler, J. Gorsline, G. Levy, S.Z. Zhang, I.E. Weston, D. Naret, B. Berner, Pharmacokinetics of metformin gastric-retentive tablets in healthy volunteers, J. Clin. Pharmacol. 41 (2001) 655–661, https://doi.org/10.1177/00912700122010546.
[20] S.A. El-Zahaby, A.A. Kassem, A.H. El-Kamel, Formulation and in vitro evaluation of size expanding gastro-retentive systems of levofloxacin hemihydrate, Int. J. Pharm. 464 (2014) 10–18, https://doi.org/10.1016/j.ijpharm.2014.01.024.
[21] K. Park, J.R. Robinson, Bioadhesive polymers as platforms for oral-controlled drug delivery: method to study bioadhesion, Int. J. Pharm. 19 (1984) 107–127, https://doi.org/10.1016/0378-5173(84)90154-6.
[22] S. Patil, G.S. Talele, Gastroretentive mucoadhesive tablet of lafutidine for controlled release and enhanced bioavailability, Drug Delivery 22 (2015) 312–319, https://doi.org/10.3109/10717544.2013.877099.
[23] B. Singh, B. Garg, R. Bhatowa, R. Kapil, S. Saini, S. Beg, Systematic development of a gastroretentive fixed dose combination of lamivudine and zidovudine for increased patient compliance, J. Drug Delivery Sci. Technol. 37 (2017) 204–215, https://doi.org/10.1016/j.jddst.2016.12.014.
[24] C. Zhang, J. Tang, D. Liu, X. Li, L. Cheng, X. Tang, Design and evaluation of an innovative floating and bioadhesive multiparticulate drug delivery system based on hollow structure, Int. J. Pharm. 503 (2016) 41–55, https://doi.org/10.1016/j.ijpharm.2016.02.045.
[25] I. Jiménez-Martínez, T. Quirino-Barreda, L. Villafuerte-Robles, Sustained delivery of captopril from floating matrix tablets, Int. J. Pharm. 362 (2008) 37–43, https://doi.org/10.1016/j.ijpharm.2008.05.040.
[26] S. Bandari, C. Eaga, A. Thadishetty, M. Yamsani, Formulation and evaluation of multiple tablets as a biphasic gastroretentive floating drug delivery system for fenoverine, Acta Pharmaceutica 60 (2010), https://doi.org/10.2478/v10007-010-0001-3.
[27] F. Eisenächer, G. Garbacz, K. Mäder, Physiological relevant in vitro evaluation of polymer coats for gastroretentive floating tablets, Eur. J. Pharm. Biopharm. 88 (2014) 778–786, https://doi.org/10.1016/j.ejpb.2014.07.009.
[28] M.D. Chavanpatil, P. Jain, S. Chaudhari, R. Shear, P.R. Vavia, Novel sustained release, swellable and bioadhesive gastroretentive drug delivery system for ofloxacin, Int. J. Pharm. 316 (2006) 86–92, https://doi.org/10.1016/j.ijpharm.2006.02.038.
[29] S. Sungthongjeen, P. Sriamornsak, S. Puttipipatkhachorn, Design and evaluation of floating multi-layer coated tablets based on gas formation, Eur. J. Pharm. Biopharm. 69 (2008) 255–263, https://doi.org/10.1016/j.ejpb.2007.09.013.
[30] T.-O. Oh, J.-Y. Kim, J.-M. Ha, S.-C. Chi, Y.-S. Rhee, C.-W. Park, E.-S. Park, Preparation of highly porous gastroretentive metformin tablets using a sublimation method, Eur. J. Pharm. Biopharm. 83 (2013) 460–467, https://doi.org/10.1016/j.ejpb.2012.11.009.
[31] K.-M. Hwang, C.-H. Cho, N.-T. Tung, J.-Y. Kim, Y.-S. Rhee, E.-S. Park, Release kinetics of highly porous floating tablets containing cilostazol, Eur. J. Pharm. Biopharm. 115 (2017) 39–51, https://doi.org/10.1016/j.ejpb.2017.01.027.
[32] W. Erni, K. Held, The hydrodynamically balanced system: a novel principle of controlled drug release, Eur. Neurol. 27 (1987) 21–27, https://doi.org/10.1159/000116171.
[33] J. Ali, S. Arora, A. Ahuja, A.K. Babbar, R.K. Sharma, R.K. Khar, S. Baboota, Formulation and development of hydrodynamically balanced system for metformin: in vitro and in vivo evaluation, Eur. J. Pharm. Biopharm. 67 (2007) 196–201, https://doi.org/10.1016/j.ejpb.2006.12.015.
[34] M.I. Tadros, Controlled-release effervescent floating matrix tablets of ciprofloxacin hydrochloride: development, optimization and in vitro–in vivo evaluation in healthy human volunteers, Eur. J. Pharm. Biopharm. 74 (2010) 332–339, https://doi.org/10.1016/j.ejpb.2009.11.010.
[35] C. Zhang, M. Xu, X. Tao, J. Tang, Z. Liu, Y. Zhang, X. Lin, H. He, X. Tang, A floating multiparticulate system for ofloxacin based on a multilayer structure: In vitro and in vivo evaluation, Int. J. Pharm. 430 (2012) 141–150, https://doi.org/10.1016/j.ijpharm.2012.04.013.
[36] Q. Li, X. Guan, M. Cui, Z. Zhu, K. Chen, H. Wen, D. Jia, J. Hou, W. Xu, X. Yang, W. Pan, Preparation and investigation of novel gastro-floating tablets with 3D extrusion-based printing, Int. J. Pharm. 535 (2018) 325–332, https://doi.org/10.1016/j.ijpharm.2017.10.037.
[37] S. Kumaraswamy, S.R. Thangasundaralingam, R. Sekar, A. Jayakrishnan, A floating-type dosage form of repaglinide in polycarbonate microspheres, J. Drug Delivery Sci. Technol. 41 (2017) 99–105, https://doi.org/10.1016/j.jddst.2017.07.005.
[38] E. Losi, R. Bettini, P. Santi, F. Sonvico, G. Colombo, K. Lofthus, P. Colombo, N.A. Peppas, Assemblage of novel release modules for the development of adaptable drug delivery systems, J. Control. Release 111 (2006) 212–218, https://doi.org/10.1016/j.jconrel.2005.12.006.
[39] Y. Hattori, M. Otsuka, NIR spectroscopic study of the dissolution process in pharmaceutical tablets, Vib. Spectrosc. 57 (2011) 275–281, https://doi.org/10.1016/j.vibspec.2011.09.003.
[40] M.A. Repka, S.K. Battu, S.B. Upadhye, S. Thumma, M.M. Crowley, F. Zhang, C. Martin, J.W. McGinity, Pharmaceutical applications of hot-melt extrusion: part II, Drug Dev. Ind. Pharm. 33 (2007) 1043–1057, https://doi.org/10.1080/03639040701525627.
[41] J. Breitenbach, Melt extrusion: from process to drug delivery technology, Eur. J. Pharm. Biopharm. 54 (2002) 107–117.
[42] M. Fukuda, N.A. Peppas, J.W. McGinity, Floating hot-melt extruded tablets for gastroretentive controlled drug release system, J. Control. Release 115 (2006) 121–129, https://doi.org/10.1016/j.jconrel.2006.07.018.
[43] A.Q. Vo, X. Feng, J.T. Morott, M.B. Pimparade, R.V. Tiwari, F. Zhang, M.A. Repka, A novel floating controlled release drug delivery system prepared by hot-melt extrusion, Eur. J. Pharm. Biopharm. 98 (2016) 108–121, https://doi.org/10.1016/j.ejpb.2015.11.015.
[44] K. Nakamichi, H. Yasuura, H. Fukui, M. Oka, S. Izumi, Evaluation of a floating dosage form of nicardipine hydrochloride and hydroxypropylmethylcellulose acetate succinate prepared using a twin-screw extruder, Int. J. Pharm. 218 (2001) 103–112, https://doi.org/10.1016/S0378-5173(01)00617-2.
[45] A.Q. Vo, X. Feng, M. Pimparade, X. Ye, D.W. Kim, S.T. Martin, M.A. Repka, Dual-mechanism gastroretentive drug delivery system loaded with an amorphous solid dispersion prepared by hot-melt extrusion, Eur. J. Pharm. Sci. 102 (2017) 71–84, https://doi.org/10.1016/j.ejps.2017.02.040.
[46] G.G. Graham, J. Punt, M. Arora, R.O. Day, M.P. Doogue, J.K. Duong, T.J. Furlong, J.R. Greenfield, L.C. Greenup, C.M. Kirkpatrick, J.E. Ray, P. Timmins, K.M. Williams, Clinical pharmacokinetics of metformin, Clin Pharmacokinet. 18 (2011).
[47] W.R. Proctor, D.L. Bourdet, D.R. Thakker, Mechanisms underlying saturable intestinal absorption of metformin, Drug Metab. Dispos. 36 (2008) 1650–1658, https://doi.org/10.1124/dmd.107.020180.
[48] L.J. McCreight, C.J. Bailey, E.R. Pearson, Metformin and the gastrointestinal tract, Diabetologia 59 (2016) 426–435, https://doi.org/10.1007/s00125-015-3844-9.
[49] P.H. Marathe, Y. Wen, J. Norton, D.S. Greene, R.H. Barbhaiya, I.R. Wilding, Effect of altered gastric emptying and gastrointestinal motility on metformin absorption: metformin absorption with altered gastrointestinal transit, Br. J. Clin. Pharmacol. 50 (2001) 325–332, https://doi.org/10.1046/j.1365-2125.2000.00264.x.
[50] B. Berner, V.E. Cowles, Case studies in swelling polymeric gastric retentive tablets, Exp. Opinion Drug Delivery 3 (2006) 541–548, https://doi.org/10.1517/17425247.3.4.541.
[51] A.K. Lalloo, E.L. McConnell, L. Jin, R. Elkes, C. Seiler, Y. Wu, Decoupling the role of image size and calorie intake on gastric retention of swelling-based gastric retentive formulations: Pre-screening in the dog model, Int. J. Pharm. 431 (2012) 90–100, https://doi.org/10.1016/j.ijpharm.2012.04.044.
[52] V.M. Riedel, Kontinuierliche Feuchtgranulation im Zweischneckenextruder, 1. Auflage, Verlag Dr. Hut München, 2016.
[53] C.A. Schneider, W.S. Rasband, K.W. Eliceiri, NIH image to ImageJ: 25 years of image analysis, Nat. Methods 9 (2012) 671–675, https://doi.org/10.1038/nmeth.2089.
[54] J. Schindelin, I. Arganda-Carreras, E. Frise, V. Kaynig, M. Longair, T. Pietzsch, S. Preibisch, C. Rueden, S. Saalfeld, B. Schmid, J.-Y. Tinevez, D.J. White, V. Hartenstein, K. Eliceiri, P. Tomancak, A. Cardona, Fiji: an open-source platform for biological-image analysis, Nat. Methods 9 (2012) 676–682, https://doi.org/10.1038/nmeth.2019.
[55] D. Desai, B. Wong, Y. Huang, Q. Ye, D. Tang, H. Guo, M. Huang, P. Timmins, Surfactant-mediated dissolution of metformin hydrochloride tablets: wetting effects versus ion pairs diffusivity, J. Pharm. Sci. 103 (2014) 920–926, https://doi.org/10.1002/jps.23852.
[56] FDA, Dissolustion testing of immediate release dosage forms, Guidance for Industry (1997), https://www.fda.gov/.
[57] D.A. Diaz, S.T. Colgan, C.S. Langer, N.T. Bandi, M.D. Likar, L. Van Alstine, Dissolution similarity requirements: how similar or dissimilar are the global regulatory expectations? AAPS J. 18 (2016) 15–22, https://doi.org/10.1208/s12248-015-9830-9.
[58] J. Timmermans, A.J. Moës, How well do floating dosage forms float? Int. J. Pharm. 62 (1990) 207–216, https://doi.org/10.1016/0378-5173(90)90234-U.
[59] K. Kosmidis, P. Argyrakis, P. Macheras, Fractal kinetics in drug release from finite fractal matrices, J. Chem. Phys. 119 (2003) 6373–6377, https://doi.org/10.1063/1.1603731.
[60] K. Kosmidis, P. Argyrakis, P. Macheras, A reappraisal of drug release laws using Monte Carlo simulations: the prevalence of the Weibull function, Pharm. Res. 20 (2003) 988–995.
[61] M. Koziolek, M. Grimm, F. Schneider, P. Jedamzik, M. Sager, J.-P. Kühn, W. Siegmund, W. Weitschies, Navigating the human gastrointestinal tract for oral drug delivery: uncharted waters and new frontiers, Adv. Drug Deliv. Rev. 101 (2016) 75–88, https://doi.org/10.1016/j.addr.2016.03.009.
[62] D. Cassilly, S. Kantor, L.C. Knight, A.H. Maurer, R.S. Fisher, J. Semler, H.P. Parkman, Gastric emptying of a non-digestible solid: assessment with simultaneous SmartPill pH and pressure capsule, antroduodenal manometry, gastric emptying scintigraphy: gastric emptying of a non-digestible capsule, Neurogastroenterol. Motility 20 (2008) 311–319, https://doi.org/10.1111/j.1365-2982.2007.01061.x.
[63] P. Mojaverian, R.K. Ferguson, P.H. Vlasses, M.L. Rocci, A. Oren, J.A. Fix, L.J. Caldwell, C. Gardner, Estimation of gastric residence time of the heidelberg capsule in humans: effect of varying food composition, Gastroenterology 89 (1985) 392–397, https://doi.org/10.1016/0016-5085(85)90342-7.
[64] B. Laulicht, A. Tripathi, V. Schlageter, P. Kucera, E. Mathiowitz, Understanding gastric forces calculated from high-resolution pill tracking, Proc. Natl. Acad. Sci. 107 (2010) 8201–8206, https://doi.org/10.1073/pnas.1002292107.
[65] L. Whitehead, J.T. Fell, J.H. Collett, H.L. Sharma, A.-M. Smith, Floating dosage forms: an in vivo study demonstrating prolonged gastric retention, J. Control. Release 55 (1998) 3–12, https://doi.org/10.1016/S0168-3659(97)00266-6.
[66] N. Mazer, E. Abisch, J.-C. Gfeller, R. Laplanche, P. Bauerfeind, M. Cucala, M. Lukachich, A. Blum, Intragastric behavior and absorption kinetics of a normal and "floating" modified-release capsule of Isradipine under fasted and fed conditions, J. Pharm. Sci. 77 (1988) 647–657, https://doi.org/10.1002/jps.2600770802.
[67] A. Holwerda, K. Lenaerts, J. Bierau, L. van Loon, Body position modulates gastric emptying and affects the post-prandial rise in plasma amino acid concentrations following protein ingestion in humans, Nutrients 8 (2016) 221, https://doi.org/10.3390/nu8040221.
[68] Y. Imai, I. Kobayashi, S. Ishida, T. Ishikawa, M. Buist, T. Yamaguchi, Antral

recirculation in the stomach during gastric mixing, Am. J. Physiol.-Gastrointestinal Liver Physiol. 304 (2013) G536–G542, https://doi.org/10.1152/ajpgi.00350.2012.
[69] J.D. Bonny, H. Leuenberger, Matrix type controlled release systems II. Percolation effects in non-swellable matrices, Pharmaceutica Acta Helvetiae 68 (1993) 25–33, https://doi.org/10.1016/0031-6865(93)90005-Q.
[70] H. Leuenberger, J.D. Bonny, M. Kolb, Percolation effects in matrix-type controlled drug release systems, Int. J. Pharm. 115 (1995) 217–224, https://doi.org/10.1016/0378-5173(94)00266-8.
[71] M. Maus, Computer unterstützte Arzneiformenentwicklung am Beispiel schmelzextrudierter Matrix-Retardpellets auf Basis eines kationischen Polymethacrylats, Eberhard Karls Universität, 2007.
[72] J.B. Dressman, R.R. Berardi, L.C. Dermentzoglou, T.L. Russell, S.P. Schmaltz, J.L. Bamett, K.M. Jarvenpaa, Upper gastrointestinal (GI) pH in young, healthy men and women, Pharm. Res. (1990) 6.
[73] T.L. Russell, R.R. Berardi, J.L. Barnett, L.C. Dermentzoglou, K.M. Jarvenpaa, S.P. Schmaltz, J.B. Dressman, Upper gastrointestinal pH in seventy-nine healthy, elderly, North American men and women, Pharm. Res. 10 (1993) 187–196.